PHOTOSYNTHETICA
International Journal for Photosynthesis Research

DOI 10.32615/ps.2022.035 PHOTOSYNTHETICA 60 (4): 489-496, 2022

Detection of antibiotic and microplastic pollutants in *Chrysanthemum coronarium* L. based on chlorophyll fluorescence

M.Y. ZHONG[*,†], K.Y. KHAN[*,**,†], L.J. FU[*], Q. XIA[*], H. TANG[***], H.J. QU[*], S. YUAN[*], J.L. TAN[#], and Y. GUO[*,+]

Key Laboratory of Advanced Process Control for Light Industry, Ministry of Education, Jiangnan University, 214122 Wuxi, China[*]
Institute of Environment and Ecology, Institute of Environmental Health and Ecological Security, School of the Environment and Safety Engineering, Jiangsu University, Zhenjiang, China[**]
Lushixin Sci. & Tec. (Wuxi) Co. Ltd., 214124 Wuxi, China[***]
Department of Bioengineering, University of Missouri, Columbia, MO 65211, USA[#]

Abstract

Large amounts of antibiotics and microplastics are used in daily life and agricultural production, which affects not only plant growth but also potentially the food safety of vegetables and other plant products. Fast detection of the presence of antibiotics and microplastics in leafy vegetables is of great interest to the public. In this work, a method was developed to detect sulfadiazine and polystyrene, commonly used antibiotics and microplastics, in vegetables by measuring and modeling photosystem II chlorophyll *a* fluorescence (ChlF) emission from leaves. *Chrysanthemum coronarium* L., a common beverage and medicinal plant, was used to verify the developed method. Scanning electron microscopy, transmission electron microscopy, and liquid chromatograph-mass spectrometer analysis were used to show the presence of the two pollutants in the samples. The developed kinetic model could describe measured ChlF variations with an average relative error of 0.6%. The model parameters estimated for the chlorophyll *a* fluorescence induction kinetics curve (OJIP) induction can differentiate the two types of stresses while the commonly used ChlF OJIP induction characteristics cannot. This work provides a concept to detect antibiotic pollutants and microplastic pollutants in vegetables based on ChlF.

Keywords: antibiotics; food security; microplastics; modeling; OJIP transients; vegetable quality detection.

Highlights

- A model structure was proposed to describe chlorophyll *a* fluorescence from leaves
- Model parameter estimates can differentiate antibiotic and microplastic pollutants
- The method is sensitive for antibiotic and microplastic detection

Received 14 April 2022
Accepted 26 July 2022
Published online 20 September 2022

[+]Corresponding author
e-mail: guoy@jiangnan.edu.cn

Abbreviations: ChlF – chlorophyll *a* fluorescence; F_i – chlorophyll *a* fluorescence intensity at the I step; F_j – chlorophyll *a* fluorescence intensity at the J step; F_m – maximal fluorescence yield of the dark-adapted state; F_m/F_o – electron transport through PSII; F_o – minimal fluorescence yield of the dark-adapted state; F_v – variable fluorescence (= $F_m - F_o$); F_v/F_m – maximal quantum yield of PSII photochemistry; F_v/F_o – quantum efficiency of photosystem II; M_o – approximate initial slope (in ms^{-1}) of fluorescence transient [= $4(F_{300} - F_o)/(F_m - F_o)$]; OJIP – chlorophyll *a* fluorescence induction kinetics curve; PQ – plastoquinone; PQH_2 – plastoquinol; PS – polystyrene; SDZ – sulfadiazine; V_i – relative variable fluorescence intensity at the I step [= $(F_i - F_o)/(F_m - F_o)$]; V_j – relative variable fluorescence intensity at the J step [= $(F_j - F_o)/(F_m - F_o)$].

Acknowledgments: This project is partially supported by the National Natural Science Foundation of China (51961125102, 31771680), and the 111 Project (B12018).

[†]These authors contributed equally.

Conflict of interest: The authors declare that they have no conflict of interest.

Introduction

Two emerging pollutants in agriculture, antibiotics and microplastics, have attracted extensive attention all over the world (Ezugworie *et al.* 2021, Rehm *et al.* 2021). Microplastics usually refer to plastic particles with a particle size lesser than 5 mm (Peez *et al.* 2019). With the massive use of these products, microplastics do not only widely exist in water and soil but also accumulate in the natural environment through sewage, rain, and food chains owing to their small size and non-degradability, which may cause serious impacts on human health (Li *et al.* 2021a). Similarly, antibiotics also have the problems of slow degradation and accumulation (Lin *et al.* 2021). It has been confirmed that most antibiotics will be excreted in the urine and feces of patients or animals in the form of original or active metabolites, and then enter the water or soil environment for long-term retention (Ezugworie *et al.* 2021). When humans and animals consume vegetables grown in contaminated soil or water, antibiotics and microplastics are very likely to pose a serious threat to human health directly or indirectly. Therefore, it is very important to develop effective methods for the detection of antibiotics and microplastics in vegetables.

Sulfadiazine (SDZ) is one of the most commonly used sulfonamide antibiotics in clinical practice (Xiang *et al.* 2021). Because of its potency and low cost, it is often used to treat and resist bacterial infections such as meningitis and upper respiratory system infections (Joseph and Kumar 2010). Different types of vegetables exhibit different effects of sulfa antibiotics (Li *et al.* 2010). Studies have shown the effect of enrichment of SDZ in *Brassica chinensis* L. and *Lactuca sativa* var. *longifolia* Lam. is obvious, and it leads to different degrees of chlorophyll (Chl) content reduction in vegetables (Si *et al.* 2017, Li *et al.* 2021b). According to Khan *et al.* (2021) and Liu *et al.* (2018) different antibiotics accumulated in *Brassica chinensis* L. and ginger and had a negative impact on their chlorophyll fluorescence.

Polystyrene (PS) is one of the most common microplastics and is often used in the manufacture of transparent plastic products such as food and commodity packaging and laboratory utensils (Zhang *et al.* 2018, Gu *et al.* 2020). It has been demonstrated that PS microplastic particles may transfer from roots to stems and leaves with transpiration flow through the vascular system of plants (Li *et al.* 2019). These PS microplastic particles are toxic and can be absorbed by the human intestinal tract, causing hemolysis when they come into direct contact with red blood cells. In high concentrations, PS particles induce local inflammation in tissues (Stock *et al.* 2019, Hwang *et al.* 2020). SDZ and PS, which are slow to degrade and gradually accumulate, are likely to become potential threats to human health. These two pollutants are very common in soil and will coexist for a long time in the future. Detection of these two pollutants is therefore very important.

Detection of antibiotics and microplastics has mainly relied on chemical methods, such as high-performance liquid chromatography (HPLC), liquid chromatography-tandem mass spectrometry (LC-MS/MS), pyrolysis gas chromatography-mass spectrometry (Py-GC-MS), or spectral analysis methods such as Fourier transform infrared spectroscopy (FT-IR) and Raman spectroscopy (Fan *et al.* 2019, Qi *et al.* 2019). The costs and requirements of sophisticated lab instruments make these methods impractical for routine use. The handheld chlorophyll fluorometer, on the other hand, is a portable, highly accurate, and cost-effective instrument that can identify plant stresses from PSII ChlF. As an effective probe for measuring plant photosynthetic activity, PSII ChlF has been widely used because of its non-destructive, accurate, and sensitive characteristics. Therefore, it is of great significance to study whether ChlF can be used for detecting antibiotic and microplastic pollutants in leafy vegetables.

Studies have shown that environmental stresses may change the shape of ChlF induction (Li *et al.* 2013, Fu *et al.* 2019a). However, there are still difficulties in distinguishing multiple pollutants from the response of ChlF. Therefore, it is desirable to develop a method to differentiate antibiotic and microplastic pollution in vegetables based on ChlF. Mechanistic models of ChlF have been widely established at different levels of complexity (Zhu *et al.* 2005, Guo and Tan 2011, Stirbet and Govindjee 2016, Fu *et al.* 2019a). These models can be used to describe the responses of ChlF to changes in different environmental and plant physiological factors, such as photosynthetic active radiation, temperature, and external stresses. Generally, external stresses will cause changes in the reaction rate of the photosynthetic system, which will lead to ChlF variations. Reaction rates estimated from ChlF signals may thus be used to differentiate antibiotic and microplastic pollutants in vegetables if they have different impacts on plants biologically. In this study, a model structure for PSII ChlF was developed. ChlF from *Chrysanthemum coronarium* L. (control, SDZ-stressed group, and PS-stressed group) was measured. Model parameters were estimated from measured ChlF signals and used to differentiate the three groups.

Materials and methods

Model development: The photochemical reactions of PSII, including electron transport, consist of steps beginning with light absorption to the generation of ATP (Fu *et al.* 2019b). A photon is first absorbed by an antenna chlorophyll (Chl) molecule and excites one electron. The energy of the excited electron transfers the photon energy to a PSII reaction center and the excited electron is passed to plastoquinone (PQ), named Q_A (bound tightly on the D2 protein), and reduces Q_A through the acceptor of PSII, named pheophytin. In turn, the electron on Q_A^- is transferred to another plastoquinone molecule, named Q_B (bound to the D1 protein), and reduces Q_B. When Q_B receives two electrons one by one, all originating from the oxidation of water molecules, Q_B^{2-} will accept two protons to form plastoquinol PQH_2 and diffuse away from the Q_B site. A PQ molecule from a PQ pool will refill the

empty Q_B site and becomes a new Q_B. Finally, the PQH_2 will be back to the PQ pool through the Q-cycle (Ebenhöh *et al.* 2014). The electron transferring processes before Q_A is very fast and is usually ignored in the modeling process for simplicity as done in the literature (Zhu *et al.* 2005, Guo and Tan 2011, Fu *et al.* 2019b). According to the first- or second-order chemical reaction kinetics, the main chemical reactions can thus be represented by Eqs. 1–5.

$$Q_A \underset{k_2}{\overset{k_1}{\rightleftarrows}} Q_A^- \tag{1}$$

$$Q_A^- + Q_B \underset{k_4}{\overset{k_3}{\rightleftarrows}} Q_A + Q_B^- \tag{2}$$

$$Q_A^- + Q_B^- \underset{k_6}{\overset{k_5}{\rightleftarrows}} Q_A + Q_B^{2-} \tag{3}$$

$$Q_B^{2-} + PQ \xrightarrow{k_7} Q_B + PQH_2 \tag{4}$$

$$PQH_2 \xrightarrow{k_8} PQ \tag{5}$$

The total probability for Q_A (Q_A or Q_A^-) to exist and that for Q_B (Q_B, Q_B^-, or Q_B^{2-}) at one reaction center can be set to 1 (Guo and Tan 2011). The PQ pool exists in two forms (PQ and PQH_2) and the pool size is a constant PQ_0. Q_A^-, Q_B^-, Q_B^{2-}, and PQH_2 are selected as the state variables. k_1 to k_8 are chemical reaction rates.

State variable	Values	Initial concentration
Q_A^-	y_1	0
Q_B^-	y_2	0
Q_B^{2-}	y_3	0
PQH_2	y_4	0

y_1 through y_4 are used to denote the probability or concentration of the four state variables. Differential equations can thus be developed to describe the chemical reaction kinetics represented by Eqs. 1 to 5 as follows.

$$\frac{dy_1}{dt} = k_1(1-y_1) - k_2 y_1 - k_3 y_1(1-y_2-y_3) + k_4(1-y_1)y_2 - \\ -k_5 y_1 y_2 + k_6(1-y_1)y_3 \tag{6}$$

$$\frac{dy_2}{dt} = k_3 y_1(1-y_2-y_3) - k_4(1-y_1)y_2 - k_5 y_1 y_2 + k_6(1-y_1)y_3 \tag{7}$$

$$\frac{dy_3}{dt} = k_5 y_1 y_2 - k_6(1-y_1)y_3 - k_7 y_3(PQ_0 - y_4) \tag{8}$$

$$\frac{dy_4}{dt} = k_7 y_3(PQ_0 - y_4) - k_8 y_4 \tag{9}$$

After absorption of photons by the antenna molecules, there are three pathways for the deactivation of excited Chl molecules: excitation energy transfer leading to photochemical reactions (in the reaction centers), heat generation, and fluorescence emission. The fluorescence emission efficiency can be presented by Eq. 10 according to chemical reaction kinetics as

$$F = k_9 \frac{K_f}{K_p(1-Q_A^-) + K_f + K_d} Q_A^- \tag{10}$$

where K_f, K_p, and K_d are rate constants for fluorescence emission, photochemical reactions, and heat generation, respectively, and $K_f = 6.9 \times 10^7$, $K_p = 2.6 \times 10^9$, $K_d = 4.88 \times 10^8$ (Antal *et al.* 2013), k_9 is for instrumentation gain.

Chemicals and reagents: Analytical-grade SDZ (molecular formula: $C_{10}H_{10}N_4O_2S$) was purchased from *TargetMol* (USA), and 200-μm PS [molecular formula: $(C_8H_8)_n$] was purchased from *Goose Technology Co.*, *Ltd.* (Tianjin, China).

Experimental samples: Three identical (18 × 32 × 10 cm) plastic containers were prepared and 7 kg of clean soil was added to each container. Based on detected concentrations found in the literature (Chen *et al.* 2019, Sobhani *et al.* 2021), SDZ [10 mg kg^{-1}(soil)] and PS (4% of soil w/w) (Pflugmacher *et al.* 2020, Wang *et al.* 2020, Sajjad *et al.* 2022) were mixed into the soil of different containers marked as SDZ or PS. Soil without the addition of SDZ or PS was used as a blank control group (CK).

Chrysanthemum coronarium L. seeds were purchased from *Zhejiang Agricultural Science Seed Industry Co.* (Zhejiang, China) and planted in the prepared soils at *Wuxi Honeycomb Ecological Agriculture Co.* (Wuxi, China). *Chrysanthemum coronarium* L. was sown on 14 May and harvested on 28 June in 2021 for measurements.

Chl fluorescence: The plant samples (*Chrysanthemum coronarium* L.) were transported to the laboratory at Jiangnan University (Wuxi, China) in containers at the mature stage on the 45th day, and the ChlF measurement experiment was performed at an ambient temperature of 25°C. All the plants were grown at the same time and were used at the same development stage. Ten leaves were randomly measured for each of the three groups (CK, SDZ, and PS). Before the ChlF measurements, the leaves were dark-adapted for at least 20 min in dark-adaptation clips. ChlF was measured with a hand-held *FluorPen* (*Model FF 110*, *Photon Systems Instruments*, Czech Republic) by using the OJIP protocol and maximum continuous excitation light of 3,000 μmol(photon) m^{-2} s^{-1} (100% light intensity). The ambient photosynthetic photon flux density was between 3 and 7 μmol(photon) m^{-2} s^{-1}. ChlF was measured at the center of each leaf. Due to light adaptation issues, each leaf was measured one time.

Transmission electron microscopy (TEM), scanning electron microscopy (SEM), and liquid chromatograph-mass spectrometer (LC-MS) analysis: Fresh *Chrysanthemum coronarium* L. leaf samples were harvested for TEM and were cut into small pieces. They were immediately put into 2.5% glutaraldehyde in 0.1-M Na-K-phosphate buffer (PBS) of pH 7.2 for overnight

prefixation at 4°C. PBS of pH 7.2 was used to wash the fixed samples thrice. The samples were then post-fixed in 1% (v/v) osmium tetroxide (OsO_4) in PBS of pH 7.2 for 24 h at 4°C, and then step-by-step (30, 50, 70, 80, 90, and 100% concentrations for 10 min in each solution) dehydrated through graded ethanol solutions. The TEM samples were embedded in *Spurr*'s resin overnight. A transmission electron microscope (*TEM-1230EX*, *JEOL*, Japan) was used to view the ultrathin sections that were cut with a microtome. For the SEM, the same procedure was followed as those for TEM but after dehydration in ethanol, the treated samples were critical-point-dried with desiccators, coated with gold–palladium in *Hitachi E-1010* ion sputter for 50 s, and were observed under the scanning electron microscope (*SU-8010*, *Hitachi*, Japan). LC-MS analysis following the procedures in Li *et al.* (2014) was used to determine SDZ concentration in leaves through LC-MS/MS (*Triple Quad 5500*, *SCIEX*, USA).

Statistical analysis and model fitting: Data were analyzed by one-way analysis of variance (*ANOVA*) in *SPSS* (*SPSS Inc.*, *version 24.0*, Chicago, USA) and the significance level was set at 0.05. All the figures were drawn with *Prism* (*Graphpad Prism*, *version 8.0*, CA, USA). Levenberg–Marquart algorithm (Levenberg 1944, Marquardt 1963) was used to determine the model parameters k_1–k_9 and PQ_0 by fitting the experimental fluorescence data and the algorithm was programmed in *MATLAB* (*The MathWorks*, Natick, MA, USA).

Results

LC-MS, SEM, and TEM: Under LC-MS analysis and SEM, it was clear that SDZ and PS were present in *Chrysanthemum coronarium* L. leaves. There are different degrees of SDZ accumulation in the roots, stems, and leaves of *Chrysanthemum coronarium* L. (Table 1). As shown in Fig. 1, a few PS particles can be seen in the interspaces of the leaf cells. Through TEM, the changes in mesophyll cell ultrastructure due to SDZ and PS can be seen in Fig. 1. It has been observed that under SDZ or PS stress, the thylakoid swelled and low-density areas appeared. Whereas under SDZ stress, some clusters of particles appeared in the center of the cytoplasm and some in the cell walls and outer membranes of chloroplasts, which appeared to be SDZ. This shows that the two pollutants can be absorbed from the soil by the roots of the plants and were transported to the stems and leaves through the vascular system and transpiration flow of the plants.

Fluorescence measurements: Compared to the control group (CK), the OJIP induction curve of *Chrysanthemum coronarium* L. were affected by SDZ and PS stresses (Fig. 2). The fluorescence inductions under antibiotic stress decreased more than those under microplastic stress, indicating that the antibiotic SDZ may have a greater impact on the photosynthesis of *Chrysanthemum coronarium* L. In Fig. 2, the center curve in an error bar zone represents the mean of ten samples, and the light-colored areas above

Table 1. Sulfadiazine (SDZ) concentration in different parts of plant samples (*Chrysanthemum coronarium* L.) in SDZ experimental group under LC-MS analysis. Data are means ± standard error.

Antibiotic	Root	Stem	Leaf
SDZ [μg kg^{-1}]	4.47 ± 3.41	0.76 ± 0.34	0.90 ± 0.22

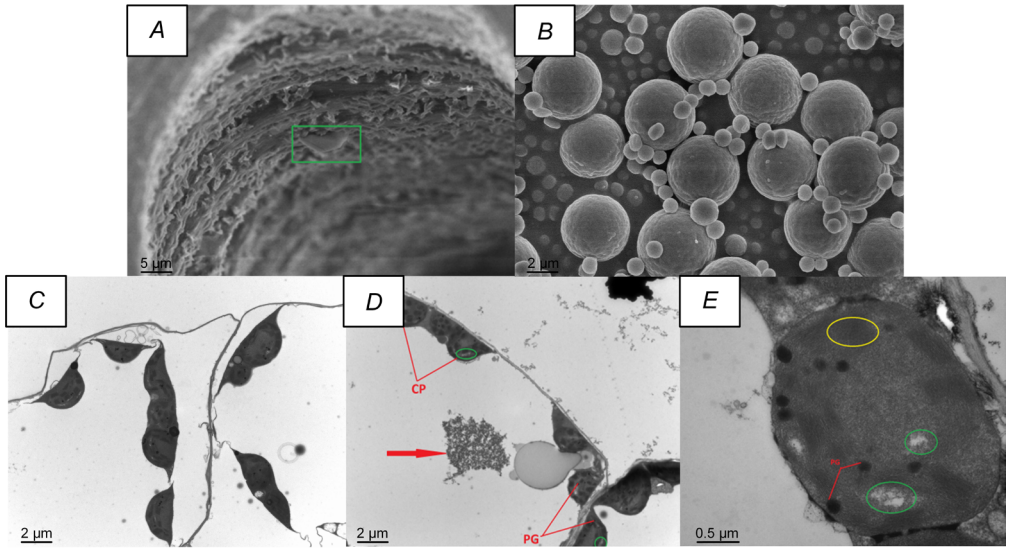

Fig. 1. Scanning electron microscopy images (*A*,*B*): (*A*) *Chrysanthemum coronarium* L. leaf treated with polystyrene; (*B*) polystyrene particles. Transmission electron microscopy images of leaves (*C*–*E*): (*C*) CK; (*D*) SDZ; (*E*) PS. CP – chloroplast; PG – plastoglobuli; yellow circle – thylakoid swelling; green circle – low-density area; green square – polystyrene particles; red arrow – SDZ clusters.

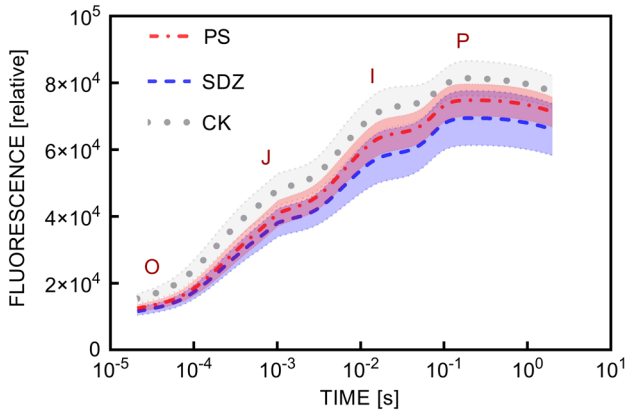

Fig. 2. Error bar graphs of OJIP inductions (PS – polystyrene-stressed group; SDZ – sulfadiazine-stressed group; CK – blank control group). One leaf was measured only once and repeated ten times by using ten different leaves for each treatment. All the plants were grown at the same time and are at the same development stage.

and below are the standard errors of the data. Despite the visible differences between the groups, it is not effective to differentiate the two types of stress by using ChlF intensity directly, as shown by the following statistical analysis of the commonly-used ChlF characteristic parameters.

Stress classification based on traditional ChlF characteristics: Conventional ChlF characteristics were compared statistically to see if they can differentiate the three treatment groups by using *ANOVA*. The ChlF characteristics analyzed include: F_o, F_j, F_i, F_m, F_v, F_m/F_o, F_v/F_o, F_v/F_m, V_i, V_j, and M_o.

Table 2 shows the *ANOVA* *p*-value between different treatments of traditional ChlF characteristics. The results show that there are significant differences in F_o, F_j, F_i, F_m, F_m/F_o, F_v/F_o, F_v/F_m, V_i, and M_o between the PS-stressed group (PS) and the control group (CK). F_v and V_j are significantly different between the SDZ-stressed group (SDZ) and the control group. However, none of the characteristics was statistically different between the PS-stressed group and the SDZ-stressed group. This indicates that the traditional ChlF characteristics are useful in detecting each of the two pollutants but cannot differentiate the two types of stresses.

Stresses classification based on model parameters: Since the pollutants affect the ChlF variations (Fig. 1), an alternative to using the conventional ChlF characteristics is to determine if the parameters in the kinetic model (Eqs. 6–10) varied consistently among the treatments. To do so, the model parameters were optimized by using the measured ChlF and the Levenberg–Marquart algorithm. Fig. 3 shows example plots comparing model predictions with measured ChlF for the three groups after model parameter optimization. It can be seen that the established model can describe the ChlF variations closely under all three conditions. The average relative

Table 2. *ANOVA* *p*-values between different treatments of traditional ChlF characteristics. * represents statistical significance at $p<0.05$, ** at $p<0.01$. PS – polystyrene-stressed group; SDZ – sulfadiazine-stressed group; CK – blank control group. F_i – chlorophyll *a* fluorescence intensity at the I step; F_j – chlorophyll *a* fluorescence intensity at the J step; F_m – maximal fluorescence yield of the dark-adapted state; F_m/F_o – electron transport through PSII; F_o – minimal fluorescence yield of the dark-adapted state; F_v – variable fluorescence ($= F_m - F_o$); F_v/F_m – maximal quantum yield of PSII photochemistry; F_v/F_o – quantum efficiency of photosystem II; M_o – approximate initial slope (in ms^{-1}) of fluorescence transient [$= 4(F_{300} - F_o)/(F_m - F_o)$]; V_i – relative variable fluorescence intensity at the I step [$= (F_i - F_o)/(F_m - F_o)$]; V_j – relative variable fluorescence intensity at the J step [$= (F_j - F_o)/(F_m - F_o)$].

	PS *vs.* CK	SDZ *vs.* CK	PS *vs.* SDZ
F_o	0.000**	0.000**	0.140
F_j	0.003**	0.000**	0.084
F_i	0.005**	0.000**	0.055
F_m	0.009**	0.001**	0.092
F_v	0.130	0.013*	0.094
F_m/F_o	0.000**	0.001**	0.855
F_v/F_o	0.000**	0.001**	0.855
F_v/F_m	0.001**	0.002**	0.796
V_j	0.063	0.042*	0.650
V_i	0.011*	0.001**	0.054
M_o	0.001**	0.003**	0.251

error for the PS, SDZ, and CK groups are 0.62, 0.62, and 0.60%, respectively.

Table 3 shows the *p*-values between different treatments of the model parameters by using *ANOVA*. The results show that parameters k_1 and k_7 show significant differences between all the three groups. That means that the control group (CK), the PS-stressed group (PS), and the SDZ-stressed group (SDZ) can be distinguished by these two parameters. Parameter k_5 shows a significant difference between the PS group and CK group and between the SDZ group and CK group, but there was no significant difference between the PS group and SDZ group, while parameter k_6 shows a significant difference between SDZ group and CK group and between PS group and SDZ group, but lacks difference between PS group and CK group. In addition, parameters k_2, k_9, PQ_0 also show significant differences between the SDZ group and CK group. The results show that the model parameters can not only detect each of the pollutants but also differentiate the two pollutants, which the conventional characteristics were unable to do.

Discussion

ChlF carries information about the physiological status of a plant and its environmental conditions (Lin *et al.* 2013, Xie *et al.* 2013). Several ChlF characteristics have been widely used to characterize plant growth performance and to detect drought stress, temperature

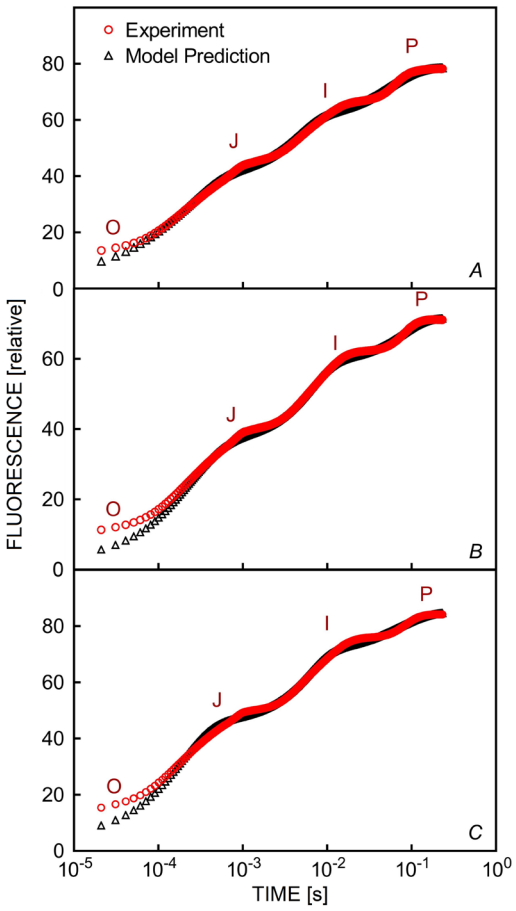

Fig. 3. Comparison of experimental data and model prediction. (*A*) Polystyrene-stressed group (PS); (*B*) sulfadiazine-stressed group (SDZ); (*C*) blank control group (CK).

Table 3. *ANOVA* *p*-values between different treatments of model parameters. * represents statistical significance at $p<0.05$, ** at $p<0.01$. PS – polystyrene-stressed group; SDZ – sulfadiazine-stressed group; CK – blank control group.

	PS *vs.* CK	SDZ *vs.* CK	PS *vs.* SDZ
k_1	0.030*	0.000**	0.042*
k_2	0.116	0.000**	0.113
k_3	0.362	0.241	0.545
k_4	0.222	0.281	0.730
k_5	0.022*	0.014*	0.526
k_6	0.575	0.021*	0.032*
k_7	0.018*	0.000**	0.012*
k_8	0.133	0.746	0.316
k_9	0.113	0.000**	0.076
PQ_0	0.061	0.020*	0.460

stress, light stress, and diseases (Wang and Guo 2005, Mandal *et al.* 2009, Sui *et al.* 2012, Lang *et al.* 2018). ChlF-based methods are simple, low-cost, and portable, and ChlF can be measured without damage to a plant (Tang *et al.* 2002, Wu *et al.* 2019). This makes ChlF an ideal signal for detecting antibiotics and microplastics in leafy vegetables.

Plant responses to abiotic stress are very complicated. Under stress conditions, plants activate their tolerance mechanism at the morphological, anatomical, cellular, and molecular levels by altering the cell ultrastructural organization through metabolic regulation. Previously, the correlation between ChlF and the ultrastructure of chloroplast has been studied for different antibiotic stresses including tetracycline and norfloxacin (Khan *et al.* 2021). Most of the past studies focused on the effects of single stress, and a few studies have explored the differences in ChlF variations under different stresses (Ye *et al.* 2014, Lotfi *et al.* 2015, Kalaji *et al.* 2016, 2018). In this study, variations were observed in leaf cell ultrastructural features including changes in the chloroplast shape and swelling of thylakoids with low-density areas under PS stress. Under SDZ stress, clusters of what appeared to be SDZ particles appeared in the cytoplasm and on the border of cell walls, and the thylakoids swelled with low-density areas and increased in the number of plastoglobuli and mitochondria (Fig. 1), which shows that plants are sensitive to microplastic and antibiotic stresses. These findings are consistent with Khan *et al.* (2021) and Zhao *et al.* (2018), who showed that antibiotics induced changes in mesophyll cells of *Brassica chinensis* L. and *Brassica parachinensis* leaves.

Accumulation of SDZ and PS in leaf tissues as observed by TEM and SEM induced alterations in cell ultrastructure and caused variations in ChlF. The traditional ChlF characteristics cannot effectively differentiate the two types of pollutants. The estimated parameters of a kinetic model based on photochemical reactions could detect each stress and differentiate the two. Compared to some complex physiological models, the model developed in this work only considers the most important reactions in PSII and the structure is thus simple with only four state variables. This is the first effort to compare traditional ChlF characteristics and model-based parameters for the detection of antibiotic and microplastic stressed vegetables, which are of important theoretical value and practical significance.

The concentration of PS in soil may accumulate with time due to PS cannot be easily degenerated. The diffusion of PS from soil to leaves is very complicated and is not only determined by PS concentration in soil. In the future, there is a need to evaluate how much PS is in soil with the exact sizes that can be absorbed by plants from the soil. Model parameters extracted from ChlF reflect effective chemical reaction rates as affected by stresses and may be used to sense environmental stresses. The ability to differentiate antibiotic and microplastic stresses is important for vegetable quality screening and is useful to consumers. In reality, many other co-occurring factors also influence PSII photochemistry, such as temperature, nutrition, water availability, genotype, *etc*. In future studies, there is a need to study the interactions among many other factors. And different vegetables may

have different biological responses to antibiotics and microplastic pollutants even at the same concentration, so performing more tests on different plants is also needed.

Conclusion: In this work, a ChlF model structure with only four state variables was developed. It can represent measured ChlF from antibiotic and microplastic stressed *Chrysanthemum coronarium* L. leaves with an average error of 0.6%. Two estimated model parameters (k_1 and k_7) showed significant differences between antibiotic and microplastic stresses while conventional ChlF characteristics cannot differentiate the two types of stresses. This work provides potential applicability for sensing SDZ and PS in vegetables. In future research, there is a need to further verify the model-based approach under the combined influence of multiple factors, such as temperature, nutrition, water availability, and genotype.

References

Antal T.K., Kovalenko H.B., Rubin A.B., Tyystjärvi E.: Photosynthesis-related quantities for education and modeling. – Photosynth. Res. **117**: 1-30, 2013.

Chen J.F., Jiang X.S., Tong T.L. *et al.*: Sulfadiazine degradation in soils: Dynamics, functional gene, antibiotic resistance genes and microbial community. – Sci. Total Environ. **691**: 1072-1081, 2019.

Ebenhöh O., Fucile G., Finazzi G. *et al.*: Short-term acclimation of the photosynthetic electron transfer chain to changing light: a mathematical model. – Philos. T. Roy. Soc. B **369**: 20130223, 2014.

Ezugworie F.N., Igbokwe V.C., Onwosi C.O.: Proliferation of antibiotic-resistant microorganisms and associated genes during composting: An overview of the potential impacts on public health, management and future. – Sci. Total Environ. **784**: 147191, 2021.

Fan Y.M., Shi J.Y., Gao L.J.: [The source and detection of microplastics in soil systems.] – Chem. Ind. Times **33**: 28-31, 2019. [In Chinese]

Fu L.J., Govindjee, Tan J.L., Guo Y.: Development of a minimized model structure and a feedback control framework for regulating photosynthetic activities. – Photosynth. Res. **146**: 213-225, 2019b.

Fu L.J., Xia Q., Tan J.L. *et al.*: Modelling and simulation of chlorophyll fluorescence from PSII of a plant leaf as affected by both illumination light intensities and temperatures. – IET Syst. Biol. **13**: 327-332, 2019a.

Gu L.Q., Tian L., Gao G. *et al.*: Inhibitory effects of polystyrene microplastics on caudal fin regeneration in zebrafish larvae. – Environ. Pollut. **266**: 114664, 2020.

Guo Y., Tan J.: Modeling and simulation of the initial phases of chlorophyll fluorescence from photosystem II. – BioSystems **103**: 152-157, 2011.

Hwang J., Choi D., Han S. *et al.*: Potential toxicity of polystyrene microplastic particles. – Sci. Rep.-UK **10**: 7391, 2020.

Joseph R., Kumar K.G.: Differential pulse voltammetric determination and catalytic oxidation of sulfamethoxazole using [5,10,15,20-tetrakis (3-methoxy-4-hydroxy phenyl) porphyrinato] Cu (II) modified carbon paste sensor. – Drug Test. Anal. **2**: 278-283, 2010.

Kalaji H.M., Jajoo A., Oukarroum A. *et al.*: Chlorophyll *a* fluorescence as a tool to monitor physiological status of plants under abiotic stress conditions. – Acta Physiol. Plant. **38**: 102, 2016.

Kalaji H.M., Rastogi A., Živčák M. *et al.*: Prompt chlorophyll fluorescence as a tool for crop phenotyping: an example of barley landraces exposed to various abiotic stress factors. – Photosynthetica **56**: 953-961, 2018.

Khan K.Y., Ali B., Shuang Z. *et al.*: Effects of antibiotics stress on growth variables, ultrastructure, and metabolite pattern of *Brassica rapa* ssp. *chinensis*. – Sci. Total Environ. **778**: 146333, 2021.

Lang Y., Wang M., Xia J.B., Zhao Q.K.: Effects of soil drought stress on photosynthetic gas exchange traits and chlorophyll fluorescence in *Forsythia suspensa*. – J. Forestry Res. **29**: 45-53, 2018.

Levenberg K.: A method for the solution of certain problems in least squares. – Quart. Appl. Math. **2**: 164-168, 1944.

Li C.C., Gan Y.D., Zhang C. *et al.*: "Microplastic communities" in different environments: Differences, links, and role of diversity index in source analysis. – Water Res. **188**: 116574, 2021a.

Li L., Zhou Q., Yin N. *et al.*: Uptake and accumulation of microplastics in an edible plant. – Chin. Sci. Bull. **64**: 928-934, 2019. [In Chinese]

Li M., Yang Z.W., Li H.J. *et al.*: [Investigation and analysis of antibiotic contamination in vegetables in Eastern Hebei.] – Contemp. Farm Mach. **3**: 54-56, 2021b. [In Chinese]

Li X.D., Xian Q.M., Liu H.L. *et al.*: [Simultaneous determination of three sulfonamides residues in vegetable by high performance liquid chromatographic method with fluorimetric detection.] – Chin. J. Anal. Chem. **38**: 429-433, 2010. [In Chinese]

Li X.W., Xie Y.F., Li C.L. *et al.*: Investigation of residual fluoroquinolones in a soil–vegetable system in an intensive vegetable cultivation area in Northern China. – Sci. Total Environ. **468-469**: 258-264, 2014.

Li X.X., Liu B.X., Guo Z.T. *et al.*: [Effects of NaCl stress on photosynthesis characteristics and fast chlorophyll fluorescence induction dynamics of *Pistacia chinensis* leaves.] – Chin. J. Appl. Ecol. **24**: 2479-2484, 2013. [In Chinese]

Lin H., Sun W.C., Yu Y.J. *et al.*: Simultaneous reductions in antibiotics and heavy metal pollution during manure composting. – Sci. Total Environ. **788**: 147830, 2021.

Lin Y.C., Hu Y.G., Ren C.Z. *et al.*: Effects of nitrogen application on chlorophyll fluorescence parameters and leaf gas exchange in naked oat. – J. Integr. Agr. **12**: 2164-2171, 2013.

Liu X., Lv Y., Xu K. *et al.*: Response of ginger growth to a tetracycline-contaminated environment and residues of antibiotic and antibiotic resistance genes. – Chemosphere **201**: 137-143, 2018.

Lotfi R., Pessarakli M., Gharavi-Kouchebagh P., Khoshvaghti H.: Physiological responses of *Brassica napus* to fulvic acid under water stress: chlorophyll *a* fluorescence and antioxidant enzyme activity. – Crop J. **3**: 434-439, 2015.

Mandal K., Saravanan R., Maiti S., Kothari I.L.: Effect of downy mildew disease on photosynthesis and chlorophyll fluorescence in *Plantago ovata* Forsk. – J. Plant Dis. Prot. **116**: 164-168, 2009.

Marquardt D.W.: An algorithm for least-squares estimation of non-linear parameters. – J. Soc. Ind. Appl. Math. **11**: 431-441, 1963.

Peez N., Janiska M.-C., Imhof W.: The first application of quantitative ^{1}H NMR spectroscopy as a simple and fast method of identification and quantification of microplastic particles (PE, PET, and PS). – Anal. Bioanal. Chem. **411**: 823-833, 2019.

Pflugmacher S., Sulek A., Mader H. *et al.*: The influence of new and artificial aged microplastic and leachates on the germination of *Lepidium sativum* L. – Plants-Basel **9**: 339,

2020.
Qi H.M., Yan H., Zhang L. *et al.*: [Research progress in determination methods of antibiotics residues in plants.] – J. Food Saf. Qual. **10**: 5098-5103, 2019. [In Chinese]
Rehm R., Zeyer T., Schmidt A., Fiener P.: Soil erosion as transport pathway of microplastic from agriculture soils to aquatic ecosystems. – Sci. Total Environ. **795**: 148774, 2021.
Sajjad M., Huang Q., Khan S. *et al.*: Microplastics in the soil environment: A critical review. – Environ. Technol. Innov. **27**: 102408, 2022.
Si X.Y., Sun M., Shi C.C. *et al.*: [Environmental behavior of sulfa antibiotics (SAs) and its effect on vegetable quality.] – Anhui Agr. Sci. Bull. **23**: 40-42, 2017. [In Chinese]
Sobhani Z., Panneerselvan L., Fang C. *et al.*: Chronic and transgenerational effects of polystyrene microplastics at environmentally relevant concentrations in earthworms (*Eisenia fetida*). – Environ. Toxicol. Chem. **40**: 2240-2246, 2021.
Stirbet A., Govindjee: The slow phase of chlorophyll *a* fluorescence induction in silico: Origin of the S–M fluorescence rise. – Photosynth. Res. **130**: 193-213, 2016.
Stock V., Böhmert L., Lisicki E. *et al.*: Uptake and effects of orally ingested polystyrene microplastic particles *in vitro* and *in vivo*. – Arch. Toxicol. **93**: 1817-1833, 2019.
Sui X.L., Mao S.L., Wang L.H. *et al.*: Effect of low light on the characteristics of photosynthesis and chlorophyll *a* fluorescence during leaf development of sweet pepper. – J. Integr. Agr. **11**: 1633-1643, 2012.
Tang J.J., Chen X., Katsuyoshi S.: Varietal differences in photosynthetic characters and chlorophyll fluorescence induction kinetics parameters among intergeneric progeny derived from *Oryza*×*Sorghum*, its parents, and hybrid rice. – J. Zhejiang Univ. Sci. **3**: 113-117, 2002.
Wang F., Zhang X., Zhang S. *et al.*: Interactions of microplastics and cadmium on plant growth and arbuscular mycorrhizal fungal communities in an agricultural soil. – Chemosphere **254**: 126791, 2020.
Wang G.L., Guo Z.F.: Effects of chilling stress on photosynthetic rate and chlorophyll fluorescence parameter in seedlings of two rice cultivars differing in cold tolerance. – Rice Sci. **12**: 187-191, 2005.
Wu Y.W., Li Q., Jin R. *et al.*: Effect of low-nitrogen stress on photosynthesis and chlorophyll fluorescence characteristics of maize cultivars with different low-nitrogen tolerances. – J. Integr. Agr. **18**: 1246-1256, 2019.
Xiang X.F., Wu L.Y., Zhu J.J. *et al.*: Photocatalytic degradation of sulfadiazine in suspensions of TiO_2 nanosheets with exposed (001) facets. – Chin. Chem. Lett. **32**: 3215-3220, 2021.
Xie Y.F., Cai X.L., Liu W.L. *et al.*: Effects of lanthanum nitrate on growth and chlorophyll fluorescence characteristics of *Alternanthera philoxeroides* under perchlorate stress. – J. Rare Earth. **31**: 823-829, 2013.
Ye B., Wu Y.B., Shao W. *et al.*: [Effects of combined stress of elevated temperature and drought and of re-watering on the photosynthetic characteristics and chlorophyll fluorescence parameters of *Broussonetia papyrifera* seedlings.] – Chin. J. Ecol. **33**: 2343-2349, 2014. [In Chinese]
Zhang H.B., Wang J.Q., Zhou B.Y. *et al.*: Enhanced adsorption of oxytetracycline to weathered microplastic polystyrene: Kinetics, isotherms and influencing factors. – Environ. Pollut. **243**: 1550-1557, 2018.
Zhao H.M., Huang H.B., Du H. *et al.*: Intraspecific variability of ciprofloxacin accumulation, tolerance, and metabolism in Chinese flowering cabbage (*Brassica parachinensis*). – J. Hazard. Mater. **349**: 252-261, 2018.
Zhu X.G., Govindjee, Baker N.R. *et al.*: Chlorophyll *a* fluorescence induction kinetics in leaves predicted from a model describing each discrete step of excitation energy and electron transfer associated with photosystem II. – Planta **223**: 114-133, 2005.